Appendix 1

Classification of sepsis patients as blood genomic endotypes: a prospective cohort study

Brendon P. Scicluna, PhD[1,2], Lonneke A. van Vught, MD[1], Aeilko H. Zwinderman, PhD[2*], Maryse A. Wiewel, MD[1], Emma E. Davenport, D.Phil[3], Katie L. Burnham, MGen[3], Peter Nürnberg, PhD[4,5,6*], Marcus J. Schultz, MD[7*], Janneke Horn, MD[7], Olaf L. Cremer, MD[8], Marc J. Bonten, MD[9*], Charles J. Hinds, MD[10*], Hector R. Wong, MD[11,12*], Julian C. Knight, DPhil[3*] and Tom van der Poll, MD[1,13*]

[1]Center for Experimental Molecular Medicine, Academic Medical Center, University of Amsterdam, Amsterdam, the Netherlands; [2]Department of Clinical Epidemiology, Biostatistics and Bioinformatics, Academic Medical Center, Amsterdam, the Netherlands; [3]Wellcome Trust Centre for Human Genetics, University of Oxford, Oxford, United Kingdom; [4]Cologne Center for Genomics, University of Cologne, Cologne, Germany; [5]Cologne Excellence Cluster on Cellular Stress Responses in Aging-Associated Diseases, University of Cologne, Cologne, Germany; [6]Center for Molecular Medicine Cologne, University of Cologne, Cologne, Germany; [7]Department of Intensive Care Medicine, Academic Medical Center, University of Amsterdam, Amsterdam, The Netherlands; [8]Department of Intensive Care Medicine, University Medical Center Utrecht, Utrecht, the Netherlands; [9]Department of Medical Microbiology, University Medical Center Utrecht, Utrecht, the Netherlands; [10]William Harvey Research Institute, Barts and The London School of Medicine, Queen Mary University, London, United Kingdom; [11]Division of Critical Care Medicine, Cincinnati Children's Hospital Medical Center and Cincinnati Children's Research Foundation, Cincinnati, OH, USA; [12]Department of Pediatrics, University of Cincinnati College of Medicine, Cincinnati, OH, USA; [13]Division of Infectious Diseases, Academic Medical Center, University of Amsterdam, Amsterdam, the Netherlands. * Full professor

Overview of Content

Supplementary Methods and Data

Patient inclusion of second validation and pediatric sepsis cohorts

Patients were included to the second validation cohort as part of the UK Genomic Advances in Sepsis (GAinS) study (NCT00131196) from 29 participating ICUs between Feb 1, 2006, and Feb 20, 2014.[1] Ethics approval was granted by national ethics committees and locally approved for individual participating centers. After obtaining informed consent from the patient or their legal representative, adult patients (aged >18 years) who were admitted to the ICU with sepsis due to community-acquired pneumonia were enrolled. Community acquired pneumonia was defined as a febrile illness associated with cough, sputum production, breathlessness, leucocytosis and radiological features of pneumonia acquired in the community or within less than 2 days of hospital admission. Exclusion criteria were: patient or legal representative unwilling or unable to give consent; patient <18 years of age; pregnancy; an advanced directive to withhold or withdraw life sustaining treatment; admission for palliative care only; or immune-compromise. Written, informed consent was obtained from all patients or a legal representative. Microbiological investigations were performed according to local policies and practices with organism(s) isolated, source and the use of serological methods recorded in the eCRF. Patients were followed up for 6 months following ICU discharge with date of death recorded.
Pediatric sepsis patients (children ≤10 years of age) admitted to the pediatric intensive care units and meeting published, pediatric-specific criteria for SIRS, sepsis, or septic shock were eligible[2]. All patients were assigned to one of these three classifications at study entry (day 1). Patients assigned to SIRS were excluded.

Microarray pre-processing

Total RNA was processed and hybridized to the human genome U219-96 array plate (Affymetrix) at the Cologne Center for Genomics, Cologne, Germany. Pre-processing and quality control was performed by using the affy method (version 1.36.1)[3]. Array data were background corrected by Robust Multi-array Average (RMA), quantiles-normalized and summarized by median-polish. The resultant 49,386 probe intensities were log-transformed and filtered by means of a 0.5 variance cutoff using the genefilter method[4]. In this way 24,646 expressed probes in at least one sample were recovered. The occurrence of non-experimental chip effects was evaluated by means of surrogate variable analysis method (version 3.4.0)[5] and corrected by the empirical Bayes method combat[6].

Consensus clustering and cluster size estimation

The most appropriate means to heighten confidence on the proper cluster size is to employ an ensemble of methods to test the quality and stability of the clusters. We used an algorithm that begins by subsampling a proportion of samples and genes implemented in the consensus cluster plus R package[7]. Each subsample was then partitioned into k clusters by agglomerative hierarchical clustering in an iterative process. We chose for 1000 iterations (or repetitions) of this process. Thus, the proportion of clustering processes in which two samples were clustered together was calculated and stored in a consensus matrix for each k, where we evaluated k=2 to k=12. Next, we computed the empirical cumulative distribution function (CDF), which displays the consensus distributions for each evaluated k (Figure S2A). The CDF plot and especially the calculated change in the area-under-the-CDF (AUCDF) curve as a function of k (Figure S2B) were used to identify the cluster size at which the distribution reaches an approximate maximum, thus indicating maximum stability. These tests showed a substantial change in the delta AUCDF from a two cluster model (k=2) to a four cluster model (k=4). The lack of any substantial change in the delta AUCDF after k=4 indicated that beyond this point partitioning was equivalent to stochastic picks rather than true cluster structure. To further heighten our confidence of the k=4 endotype model we evaluated both silhouette widths and cophenetic correlations. The former is a measure of how similar a sample is to its own cluster compared to other clusters, that is cohesion and separation. Positive silhouette widths for each cluster as well as the overall average provide an indication of sample cohesion within the respective cluster. Lastly, as shown in Figure S2C, the highest cophenetic correlation coefficient was found at k=4, which indicated that the similarities between samples grouped into four endotypes was most favorable.

Derivation of the molecular endotype biomarkers

Sepsis molecular endotype biomarkers were derived by using previously described methods.[8,9] The use of multiple tests in ratio combinations has been routinely practiced by physicians (e.g., risk stratification in cancer)[10-12]. Moreover, the relativity in gene expression provided by gene ratios has been shown to be favorable in validating microarrays using other technologies, for example qRT-PCR[8,9]. The 140 gene expression indices that encompassed the endotype classifier were assessed for the best combination that classified the discovery cohort. In this context, a combination was a two-gene expression ratio:

$$\text{endotype score} = [\text{gene}_i / \text{gene}_j]$$

Receiver operator characteristics (ROC) were assessed by using the pROC R package (version 1.5.4), with bootstrap resampled 95% confidence intervals.[13] Thresholds were derived by using the coordinates function in the pROC method, specifying the "best" coordinate along the ROC curve. Considering the multi-combinatorial strategy (140 x 139 [gene ratios] x 4 [endotypes] = 77,840 tests) significance was defined by Benjamini-Hochberg[14] adjusted $p < 0.05$ (adjusting for the 77,840 tests).

Differential gene expression and Ingenuity pathway analysis

Differential gene expression analysis was firstly performed by comparing patients stratified into each of four molecular endotypes to healthy subjects, and secondly by comparing each endotype to the other endotypes. For example the latter, Mars1 patient gene expression data were compared to "others", where Mars2, Mars3 and Mars4 endotypes were recoded to a single group (others). These supervised analyses were done by means of moderated t tests implemented in the limma method (version 3.14.4)[8,15-17]. Throughout Benjamini-Hochberg multiple comparison adjusted probabilities[14] (adjusted $p < 0.05$) defined significance. Results of the comparisons between Mars endotypes and healthy subjects were represented as volcano plots and venn-euler diagram. Ingenuity Pathway Analysis (Ingenuity Systems IPA, www.ingenuity.com) was used to identify enrichment of genes (adjusted $p<0.05$, fold expression +/- 1.5) that pertain to distinct canonical signaling pathways. The Ingenuity gene knowledgebase was selected as reference and human species specified. All other parameters were default. Significance was evaluated by Fisher's exact test adjusted p-values (adjusted $p < 0.01$). A continuous variable power/sample size calculation and considering a false discovery rate of 5%, beta error level 10% (90% power), a sample size of 48 patients per group was estimated. With respect to the analysis of sepsis patients classified as Mars endotypes relative to healthy subjects a sample size of 12 per group was estimated.

Evaluation of diagnostic performance

The diagnostic performance of the endotype scores was evaluated by ROC AUC analysis. The optimal point along the ROC AUC curve was used to generate accuracy, sensitivity, specificity, positive and negative predictive values using the pROC method. Positive likelihood ratios (LR+) were calculated by the following equation: sensitivity/(1-specificity). Negative likelihood ratios (LR-) were calculated using the equation: (1-sensitivity)/specificity.

Supplementary References

1. Davenport EE, Burnham KL, Radhakrishnan J, et al. Genomic landscape of the individual host response and outcomes in sepsis: a prospective cohort study. *The Lancet Respiratory medicine* 2016; **4**(4): 259-71.
2. Goldstein B, Giroir B, Randolph A, International Consensus Conference on Pediatric S. International pediatric sepsis consensus conference: definitions for sepsis and organ dysfunction in pediatrics. *Pediatric critical care medicine : a journal of the Society of Critical Care Medicine and the World Federation of Pediatric Intensive and Critical Care Societies* 2005; **6**(1): 2-8.
3. Gautier L, Cope L, Bolstad BM, Irizarry RA. affy - analysis of Affymetrix GeneChip data at the probe level. *Bioinformatics* 2004; **20**(3): 307-15.
4. Bourgon R, Gentleman R, Huber W. Independent filtering increases detection power for high-throughput experiments. *Proc Natl Acad Sci U S A* 2010; **107**(21): 9546-51.
5. Leek JT, Storey JD. Capturing heterogeneity in gene expression studies by surrogate variable analysis. *Plos Genetics* 2007; **3**(9): 1724-35.
6. Johnson W, Li C, Rabinovic A. Adjusting batch effects in microarray expression data using empirical Bayes methods. *Biostatistics* 2007; **8**(1): 118-27.
7. Wilkerson MD, Hayes DN. ConsensusClusterPlus: a class discovery tool with confidence assessments and item tracking. *Bioinformatics* 2010; **26**(12): 1572-3.
8. Scicluna BP, Klein Klouwenberg PM, van Vught LA, et al. A molecular biomarker to diagnose community-acquired pneumonia on intensive care unit admission. *Am J Respir Crit Care Med* 2015; **192**(7): 826-35.
9. McHugh L, Seldon TA, Brandon RA, et al. A Molecular Host Response Assay to Discriminate Between Sepsis and Infection-Negative Systemic Inflammation in Critically Ill Patients: Discovery and Validation in Independent Cohorts. *PLoS Med* 2015; **12**(12): e1001916.
10. Catalona WJ, Smith DS, Wolfert RL, et al. Evaluation of Percentage of Free Serum Prostate-Specific Antigen to Improve Specificity of Prostate-Cancer Screening. *Jama-Journal of the American Medical Association* 1995; **274**(15): 1214-20.
11. Ma XJ, Wang ZC, Ryan PD, et al. A two-gene expression ratio predicts clinical outcome in breast cancer patients treated with tamoxifen. *Cancer Cell* 2004; **5**(6): 607-16.
12. van't Veer LJ, Dai HY, van de Vijver MJ, et al. Gene expression profiling predicts clinical outcome of breast cancer. *Nature* 2002; **415**(6871): 530-6.
13. Robin X, Turck N, Hainard A, et al. pROC: an open-source package for R and S plus to analyze and compare ROC curves. *BMC Bioinformatics* 2011; **12**.
14. Benjamini Y, Hochberg Y. Controlling the False Discovery Rate - A Practical and Powerful Approach to Multiple Testing. *Journal of the Royal Statistical Society Series B-Methodological* 1995; **57**(1): 289-300.
15. Smyth GK. Limma: linear models for microarray data. In: R G, VJ C, H W, RA I, S D, eds. Bioinformatics and Computational Biology Solutions using R: Springer; 2005: 397-420.
16. van Lieshout MH, Scicluna BP, Florquin S, van der Poll T. NLRP3 and ASC Differentially Affect the Lung Transcriptome during Pneumococcal Pneumonia. *Am J Respir Cell Mol Biol* 2014; **4**(50): 699-712.
17. Scicluna BP, van Lieshout MH, Blok DC, Florquin S, van der Poll T. Modular Transcriptional Networks of the Host Pulmonary Response during Early and Late Pneumococcal Pneumonia. *Molecular medicine* 2015; **21**: 430-41.
18. Levy MM, Fink MP, Marshall JC, et al. 2001 SCCM/ESICM/ACCP/ATS/SIS International Sepsis Definitions Conference. *Crit Care Med* 2003; **31**(4): 1250-6.

Table S1. Diagnostic criteria for sepsis in adults according to 2001 International Sepsis Definitions Conference.[18]

Infection documented or suspected, and some of the following:
General variables
Fever (core temperature >38.3°C)
Hypothermia (core temperature <36°C)
Heart rate >90 min^{-1} or >2 SD above the normal value for age
Tachypnea
Altered mental status
Significant edema or positive fluid balance (>20 mL/kg over 24 hrs)
Hyperglycemia (plasma glucose >120 mg/dL or 7.7 mmol/L) in the absence of diabetes
Inflammatory variables
Leukocytosis (WBC count >12.000 μL^{-1})
Leukopenia (WBC count <4000 μL^{-1})
Normal WBC count with >10% immature forms
Plasma C-reactive protein >2 SD above the normal value
Plasma procalcitonin >2 SD above the normal value
Hemodynamic variables
Arterial hypotension (SBP <90 mm Hg, MAP <70, or an SBP decrease >40 mm Hg)
SvO_2 >70%
Cardiac index >3.5 $L \bullet min^{-1} \bullet m^{-2}$
Organ dysfunction variables
Arterial hypoxemia (PaO_2/FIO_2 <300)
Acute oliguria (urine output <0.5 $mL \bullet kg^{-1} \bullet hr^{-1}$ or 45 mmol/L for at least 2 hrs)
Creatinine increase >0.5 mg/dL
Coagulation abnormalities (INR >1.5 or aPTT >60 secs)
Ileus (absent bowel sounds)
Thrombocytopenia (platelet count <100,000 μL^{-1})
Hyperbilirubinemia (plasma total bilirubin >4 mg/dL or 70 mmol/L)
Tissue perfusion variables
Hyperlactatemia (>1 mmol/L)
Decreased capillary refill or mottling

Abbreviations: aPTT: activated partial thromboplastin time; INR: international normalized ratio; MAP: mean arterial blood pressure; SBP: systolic blood pressure; SD: standard deviation; SvO_2: mixed venous oxygen saturation; WBC: white blood cell.

Table S2: Characteristics of the discovery cohort classified as four molecular endotypes

	Mars 1	Mars 2	Mars 3	Mars 4	P value
Patients, n	90	105	71	40	
Demographics					
Age, median [Q1-Q3]	65 [56-72]	61 [48-71]	62 [54-71]	62 [49-71]	0.2
Gender, males (%)	47 (52)	54 (51)	46 (65)	19 (48)	0.22
Ethnicity, Caucasian (%)	73 (81.1%)	85 (81.0%)	58 (81.7%)	25 (62.5%)	0.24
Admission					
Infection likelihood, definite n (%)	61 (67.8)	73 (69.5)	34 (47.9)	24 (60)	0.02
Medical admission, n (%)	60 (66.7)	58 (55.2)	61 (85.9)	35 (87.5)	<0.001
Chronic comorbidity, n (%)					
None	37 (41.1)	50 (47.6)	24 (33.8)	13 (32.5)	0.21
Cardiovascular compromise	18 (20.0)	13 (12.4)	13 (18.3)	9 (22.5)	0.37
COPD	11 (12.2)	9 (8.6)	11 (15.5)	8 (20.0)	0.27
Diabetes	17 (18.9)	13 (12.4)	16 (22.5)	8 (20.0)	0.34
Hypertension	23 (25.6)	16 (15.2)	17 (23.9)	19 (25.0)	0.28
Malignancy	14 (15.6)	11 (10.5)	7 (9.9)	4 (10.0)	0.63
Renal insufficiency	9 (10.0)	12 (11.4)	13 (18.3)	7 (17.5)	0.36
Respiratory insufficiency	13 (14.4)	10 (9.5)	14 (19.7)	10 (25.0)	0.08
Charlson comorbidity index	4 [3-6]	3 [2-5]	4 [2-5]	4 [2-6]	0.07
Site of infection, n (%)					
Lung	34 (37.8)	37 (35.2)	36 (50.7)	23 (57.5)	0.03
Abdominal	29 (32.2)	35 (33.3)	13 (18.3)	2 (5.0)	0.002
Urinary	8 (8.9)	6 (5.7)	6 (8.5)	5 (12.5)	0.60
Skin	3 (3.3)	15 (14.3)	4 (5.6)	2 (5.0)	0.02
Cardiovascular	4 (4.4)	3 (2.9)	1 (1.4)	3 (7.5)	0.39
Central nervous system	-	-	2 (2.8)	3 (7.5)	0.003
Other*	12 (13.3)	9 (8.6)	9 (12.7)	2 (5.0)	0.42
Blood cells, median cells x10^9/Liter [Q1-Q3]					
Total leukocytes	13.20 [7.80-16.30]	15.55 [9.93-23.30]	14.70 [11.60-17.70]	11.60 [8.10-19.10]	0.02
Neutrophils	12.63 [8.77-14.22]	12.46 [7.26-17.68]	11.97 [9.00-14.91]	10.24 [6.80- 15.35]	0.58
Monocytes	0.95 [0.58-1.10]	0.62 [0.40-0.89]	0.93 [0.60-1.35]	0.50 [0.16- 0.91]	0.001
Lymphocytes	0.77 [0.37-1.40]	0.84 [0.53-1.38]	1.16 [0.51-1.72]	0.61 [0.24- 1.03]	0.14
Severity of disease on ICU admission					
APACHE IV Score, median [Q1-Q3]	81 [63-104]	74 [59-92]	73 [60-91]	78 [59-105]	0.37
Acute kidney injury, n (%)	44 (48.9)	54 (51.4)	19 (26.8)	15 (37.5)	0.01
Acute lung injury, n (%)	36 (40.0)	31 (29.5)	21 (29.6)	13 (32.5)	0.42
Outcome					
Length of stay, median [Q1-Q3]	4 [2-8]	4 [2-8]	4 [2-10]	4 [2-7]	0.95
ICU mortality, n (%)	28 (31.1)	13 (12.4)	9 (12.7)	8 (20.0)	0.004

	Mars 1	Mars 2	Mars 3	Mars 4	P value
Patients, n	90	105	71	40	
Hospital mortality, n (%)	39 (43.3)	28 (26.7)	20 (28.2)	13 (32.5)	0.07

Clinical characteristics of discovery cohort stratified by sepsis molecular endotypes. Abbreviations: Q1-Q3, 1st quartile-3rd quartile. APACHE IV, Acute Physiology and Chronic Health Evaluation IV. SOFA, sequential organ failure assessment. COPD, chronic obstructive pulmonary disease. * Other includes: bone joint infection, endocarditis, mediastinitis, myocarditis, ear infection, oral infection, pharyngitis, post-operative wound infection and lung abscess.

Table S3: Characteristics of the first validation cohort classified to four molecular endotypes

	Mars 1	Mars 2	Mars 3	Mars 4	P value
Patients, n	60	79	58	19	
Demographics					
Age, median [Q1-Q3]	64 [53-71]	65 [56-72]	62 [55-70]	66 [57-74]	0.58
Gender, males (%)	36 (60)	50 (63)	33 (57)	12 (63)	0.89
Ethnicity, Caucasian (%)	59 (98.3%)	77 (97.5%)	55 (94.8%)	17 (89.5%)	0.19
Admission					
Infection likelihood, definite n (%)	36 (60)	41 (51.9)	21 (36.2)	10 (52.6)	0.073
Medical admission, n (%)	105 (70.0)	112 (60.9)	109 (84.5)	53 (89.8)	<0.001
Chronic comorbidity, n (%)					
None	8 (13.3)	13 (16.5)	11 (19.0)	5 (26.3)	0.60
Cardiovascular compromise	17 (28.3)	19 (24.1)	14 (24.1)	5 (26.3)	0.94
COPD	5 (8.3)	13 (16.5)	9 (15.5)	3 (15.8)	0.55
Diabetes	15 (25.0)	17 (21.5)	9 (15.5)	4 (21.1)	0.64
Hypertension	22 (36.7)	27 (34.2)	22 (37.9)	5 (26.3)	0.81
Malignancy	22 (36.7)	30 (38.0)	20 (34.5)	2 (10.5)	0.15
Renal insufficiency	12 (20.0)	16 (20.3)	6 (10.3)	2 (10.5)	0.35
Respiratory insufficiency	6 (10.0)	14 (17.7)	10 (17.2)	3 (15.8)	0.61
Charlson comorbidity index	5 [3-6]	5 [3-6]	5 [2-6]	4 [2-6]	0.71
Site of infection, n (%)					
Lung	21 (35.0)	31 (39.2)	33 (56.9)	11 (57.9)	0.04
Abdominal	21 (35.0)	26 (32.9)	4 (6.9)	-	<0.001
Urinary	10 (16.7)	5 (6.3)	4 (6.9)	5 (26.3)	0.04
Skin	1 (1.7)	3 (3.8)	1 (1.7)	1 (5.3)	0.71
Cardiovascular	6 (10.0)	1 (1.3)	-	-	0.01
Central nervous system	-	2 (2.5)	1 (1.7)	1 (5.3)	0.49
Other*	10 (1.7%)	11 (13.9)	15 (25.9)	1 (5.3)	0.002
Blood cells, median cells x10^9/Liter [Q1-Q3]					
Total leukocytes	13.05 [8.30-18.47]	14.00 [8.10-23.55]	16.70 [11.50-21.25]	14.80 [12.10-21.75]	0.087
Neutrophils	9.60 [5.74-13.07]	12.18 [6.64-18.86]	12.46 [8.90-17.24]	12.69 [7.74-25.31]	0.061
Monocytes	0.58 [0.28-0.91]	0.56 [0.24-1.06]	0.86 [0.60-1.44]	0.57 [0.39-0.97]	0.004
Lymphocytes	0.84 [0.51-1.40]	0.75 [0.51-1.33]	1.12 [0.78-1.90]	0.66 [0.44-1.21]	0.008
Severity of disease on ICU admission					
APACHE IV Score, median [Q1-Q3]	90 [73-111]	86 [71-105]	76 [65-91]	87 [77-93]	0.05
Acute kidney injury, n (%)	18 (30.0)	24 (30.4)	10 (17.2)	3 (15.8)	0.21
Acute lung injury, n (%)	16 (26.7)	20 (25.3)	11 (19.0)	5 (26.3)	0.77
Outcome					
Length of stay, median [Q1-Q3]	8 [3-14]	5 [2-14]	5 [3-10]	6 [3-11]	0.79
ICU mortality, n (%)	17 (28.3)	13 (16.5)	6 (10.3)	1 (5.3)	0.03
Hospital mortality, n (%)	26 (43.3)	22 (27.8)	8 (13.8)	1 (5.3)	<0.001

Clinical characteristics of first validation cohort stratified by sepsis molecular endotypes. Abbreviations: Q1-Q3, 1st quartile-3rd quartile. APACHE IV, Acute Physiology and Chronic Health Evaluation IV. SOFA, sequential organ failure assessment. COPD, chronic obstructive pulmonary disease. * other includes: bone joint infection, endocarditis, mediastinitis, myocarditis, ear infection, oral infection, pharyngitis, post-operative wound infection and lung abscess.

Table S4: Characteristics of the second validation cohort classified as four molecular endotypes

	Mars1	**Mars2**	**Mars3**	**Mars4**	**p**
Patients, n	35	117	97	16	
Demographics					
gender, males (%)	17 (48.6)	60 (51.3)	57 (58.8)	11 (68.8)	0.391
age, median [Q1-Q3]	67.00 [59.00-76.00]	61.00 [49.00-72.00]	67.00 [50.00-78.00]	59.50 [55.75-74.50]	0.088
Severity of disease on ICU admission					
APACHE II, median [Q1-Q3]	17.00 [14.00-21.50]	18.00 [14.00-22.00]	17.00 [13.00-22.00]	17.50 [13.75-24.50]	0.723
Outcome					
14-day mortality, n (%)	10 (28.6)	19 (16.2)	7 (7.2)	4 (25)	0.012

Clinical characteristics of second validation cohort stratified by sepsis molecular endotypes. Abbreviations: Q1-Q3, 1st quartile-3rd quartile. APACHE II, Acute Physiology and Chronic Health Evaluation II.

Table S5: Pediatric sepsis cohort characteristics

	Pediatric sepsis USA
Patients, n	81
Demographics	
Gender, males (%)	47 (58)
Age, median [Q1-Q3]	2 [1-6]
Severity on ICU admission	
PRISM score, median [Q1-Q3]	16 [10-22]
Shock, n (%)	67 (82.7)
Outcome	
28 day mortality, n (%)	14 (17.3)

Clinical characteristics of the pediatric sepsis cohort, USA. Abbreviations: Q1-Q3, 1st quartile-3rd quartile. PRISM, pediatric risk of mortality.

Table S6: Performance characteristics of the candidate sepsis endotype biomarkers.

Discovery cohort									
endotype	biomarker	threshold	accuracy*	sensitivity*	specificity*	ppv*	npv*	LR+**	LR-**
Mars1	*BPGM:TAP2*	1.15	0.96 (0.93-0.98)	0.91 (0.85-0.96)	0.98 (0.96-0.99)	0.95 (0.9-0.99)	0.96 (0.94-0.98)	45.5	0.09
Mars2	*GADD45A:PCGF5*	1.05	0.91 (0.87-0.94)	0.93 (0.87-0.98)	0.9 (0.85-0.94)	0.83 (0.77-0.89)	0.96 (0.93-0.99)	9.3	0.08
Mars3	*AHNAK:PDCD10*	1.03	0.9 (0.87-0.94)	0.92 (0.84-0.98)	0.9 (0.85-0.94)	0.74 (0.66-0.82)	0.97 (0.95-0.99)	9.2	0.09
Mars4	*IFIT5:GLTSCR2*	0.57	0.95 (0.92-0.97)	0.97 (0.9-1)	0.95 (0.92-0.97)	0.69 (0.58-0.81)	1 (0.99-1)	19.4	0.03
First validation cohort									
subtype	biomarker	threshold	accuracy*	sensitivity*	specificity*	ppv*	npv*	LR+**	LR-**
Mars1	*BPGM:TAP2*	1.1	0.88 (0.83-0.92)	0.88 (0.8-0.95)	0.88 (0.83-0.93)	0.74 (0.65-0.82)	0.95 (0.92-0.98)	7.3	0.14
Mars2	*GADD45A:PCGF5*	0.96	0.83 (0.78-0.88)	0.8 (0.71-0.89)	0.85 (0.8-0.91)	0.76 (0.68-0.84)	0.88 (0.83-0.93)	5.3	0.24
Mars3	*AHNAK:PDCD10*	1	0.74 (0.68-0.8)	0.93 (0.86-0.98)	0.66 (0.59-0.73)	0.5 (0.45-0.57)	0.96 (0.93-0.99)	2.74	0.11
Mars4	*IFIT5:GLTSCR2*	0.48	0.88 (0.83-0.92)	0.95 (0.84-1)	0.87 (0.82-0.92)	0.42 (0.33-0.53)	0.99 (0.98-1)	7.3	0.057
Second validation cohort									
subtype	biomarker	threshold	accuracy*	sensitivity*	specificity*	ppv*	npv*	LR+**	LR-**
Mars1	*BPGM:TAP2*	0.84	0.8 (0.75-0.85)	0.94 (0.86-1)	0.78 (0.73-0.83)	0.4 (0.34-0.47)	0.99 (0.97-1)	4.3	0.077
Mars2	*GADD45A:PCGF5*	1.8	0.8 (0.75-0.85)	0.75 (0.68-0.83)	0.84 (0.78-0.89)	0.79 (0.72-0.85)	0.81 (0.76-0.86)	4.7	0.3
Mars3	*AHNAK:PDCD10*	0.72	0.73 (0.67-0.78)	0.82 (0.75-0.9)	0.67 (0.6-0.74)	0.59 (0.54-0.65)	0.87 (0.82-0.92)	2.5	0.27
Mars4	*IFIT5:GLTSCR2*	0.64	0.85 (0.81-0.89)	1 (1-1)	0.84 (0.8-0.88)	0.29 (0.24-0.36)	1 (1-1)	6.25	0

*threshold-dependent scores (95% confidence intervals). ppv, positive predictive value. npv, negative predictive value. LR+, positive likelihood ratio. LR-, negative likelihood ratio. *BPGM*, bisphosphoglycerate mutase. *TAP2*, transporter 2, ATP binding cassette subfamily B member. *GADD45A*, growth arrest and DNA damage inducible alpha. *PCGF5*, polycomb group ring finger 5. *AHNAK*, AHNAK nucleoprotein. *PDCD10*, programmed cell death 10. *IFIT5*, interferon induced protein with tetratricopeptide repeats 5. *GLTSCR2*, glioma tumor suppressor candidate region gene 2.

Figure S1

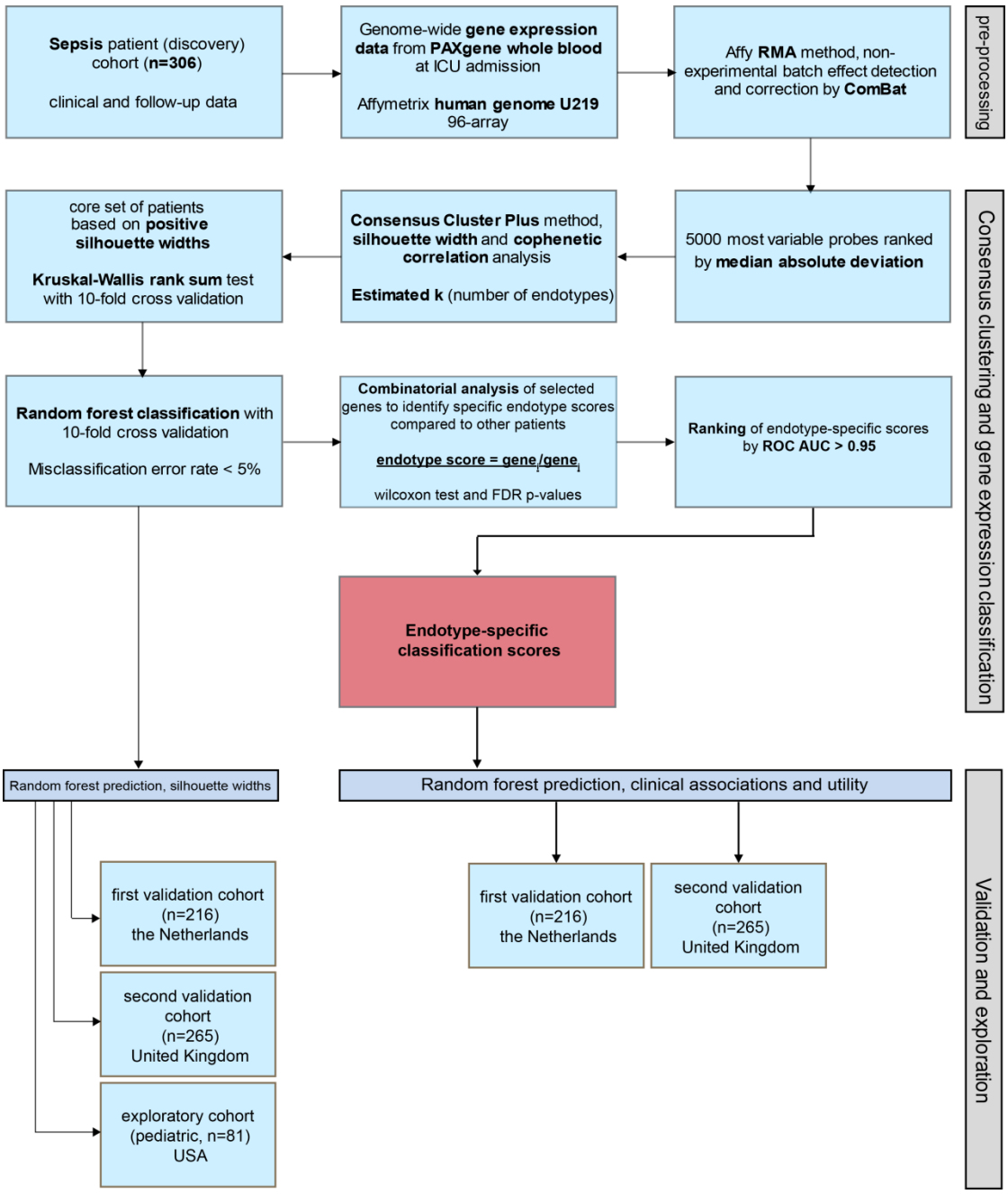

Figure S1. Methodological steps employed for the unsupervised consensus clustering and gene expression classifier construction using the discovery set and subsequent validation in independent validation datasets.

Figure S2

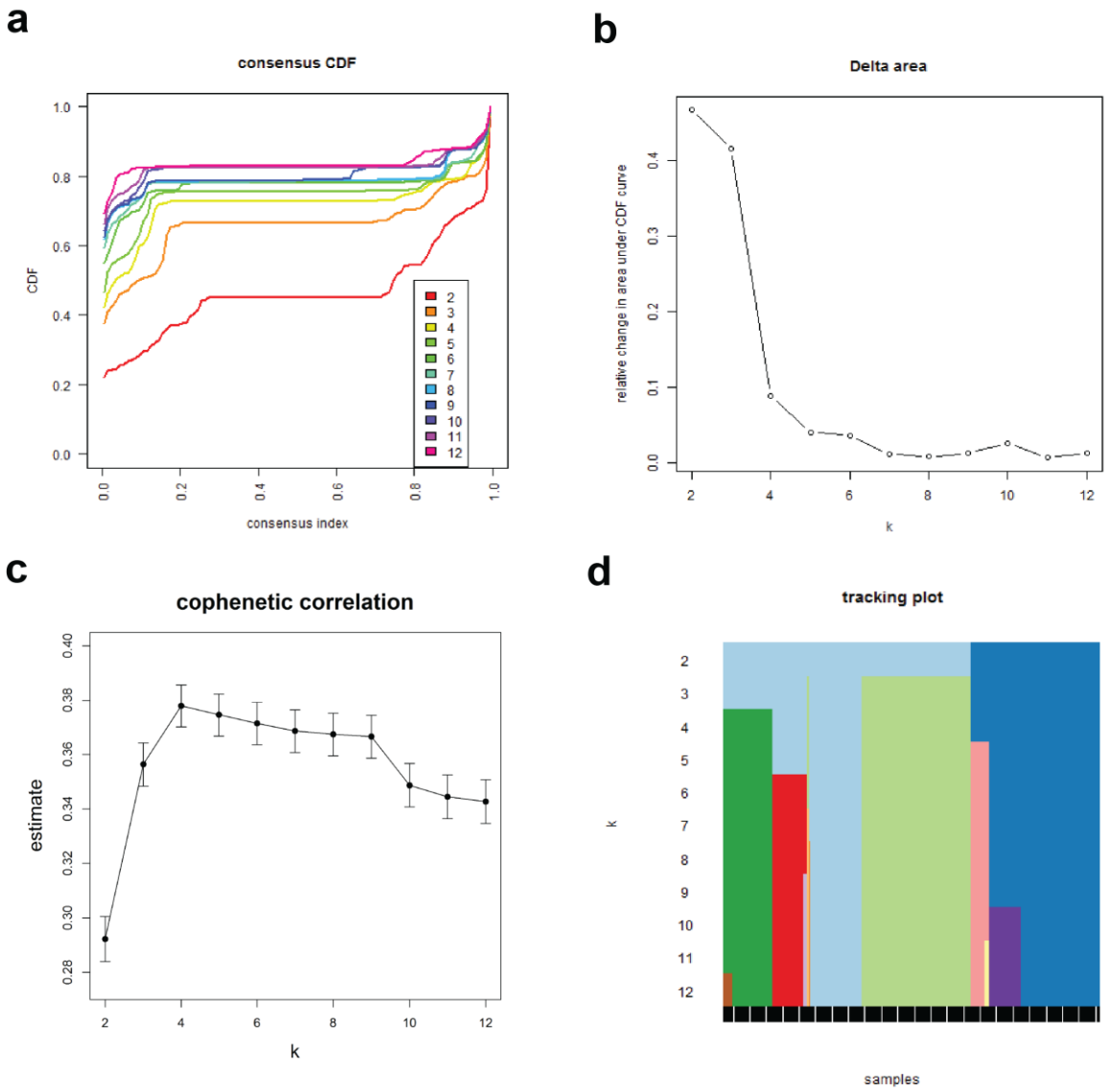

Figure S2. Unsupervised consensus cluster identification and stability in the discovery cohort (n = 306). (a) consensus cumulative distribution function (CDF) with increasing number of clusters (k2 to k12). (b) Relative change in area-under-CDF curve with increasing number of clusters (k). (c) cophenetic correlation coefficients at each cluster (k). (d) patient tracking plot that follows patients with increasing numbers of clusters (k).

Figure S3

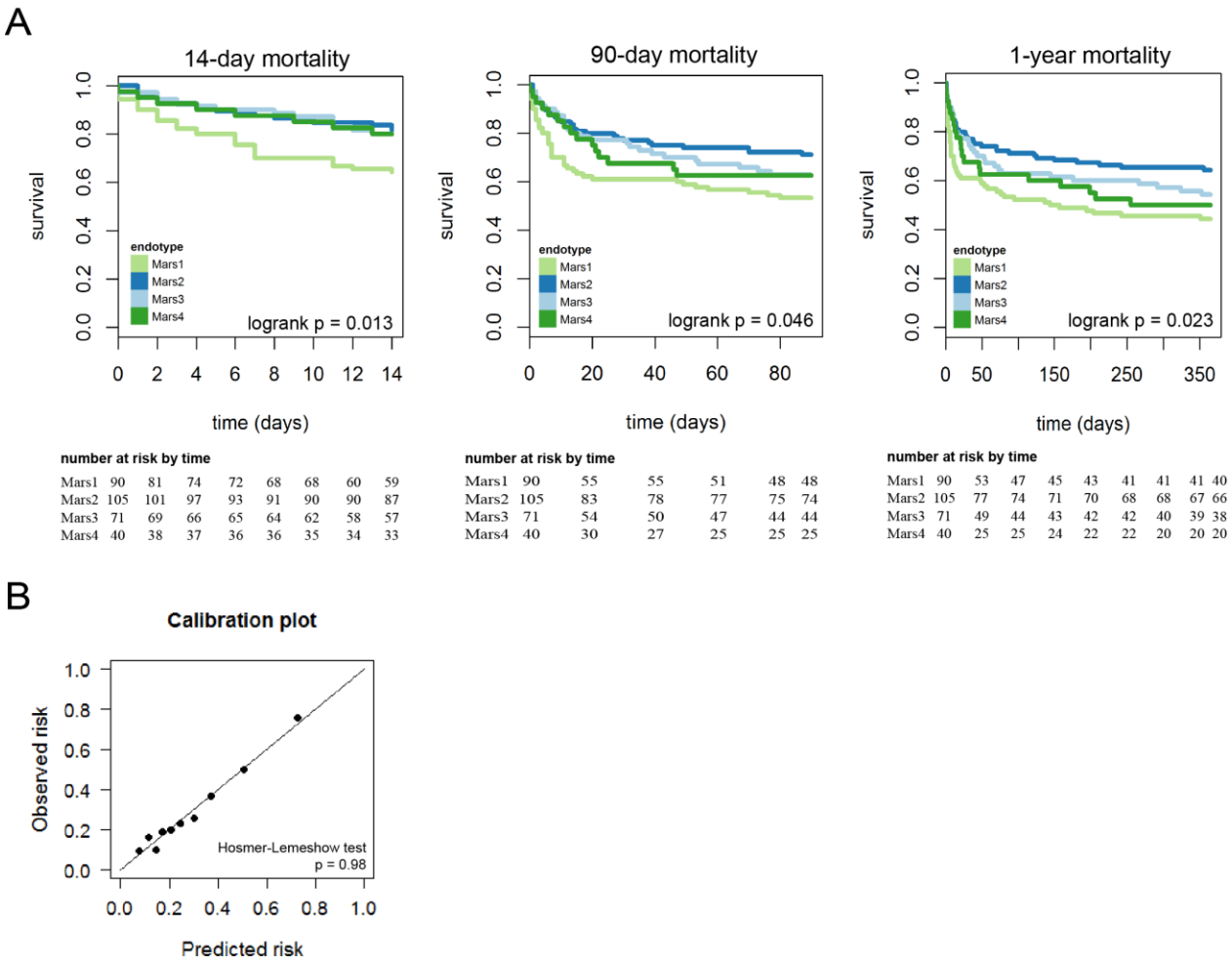

Figure S3. Mortality and net reclassification improvement (NRI) in the discovery cohort (n = 306) considering clinical and four molecular subtype models. (**A**) Patient follow-up as at 14, 90 days and 1 year with sepsis molecular endotype stratification. (**B**) Continuous NRI calibration plots of the combined Acute Physiology and Chronic Health Evaluation IV (APACHE IV) score and sepsis molecular endotypes considering 28-day mortality in discovery cohort. Plot illustrate the Hosmer-Lemeshow test probabilities, which denote optimal calibration for a continuous net reclassification assessment (p>0.05).

Figure S4

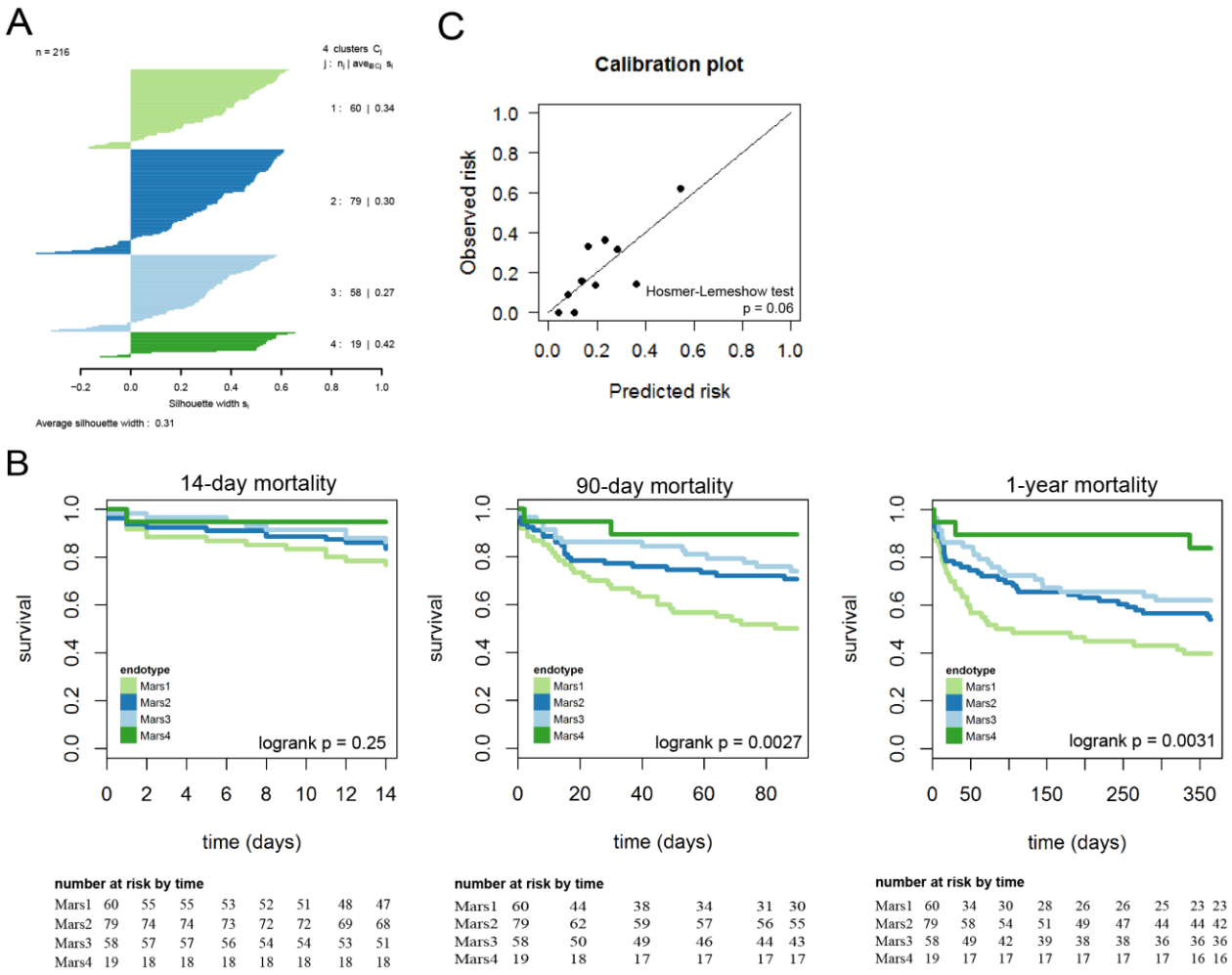

Figure S4. Molecular endotype prediction in first validation cohort from the Netherlands (n = 216). (**A**) Silhouette widths of sepsis endotype classification. (**B**) Kaplan-Meier analysis of follow-up data with sepsis endotype stratification as at 14, 90 days and 1 year. (**C**) Continuous net reclassification improvement calibration plots of the combined Acute Physiology and Chronic Health Evaluation IV (APACHE IV) score and sepsis molecular endotypes considering 28-day mortality in discovery cohort. Plot illustrate the Hosmer-Lemeshow test probabilities, which denote optimal calibration for a continuous net reclassification assessment ($p>0.05$).

Figure S5

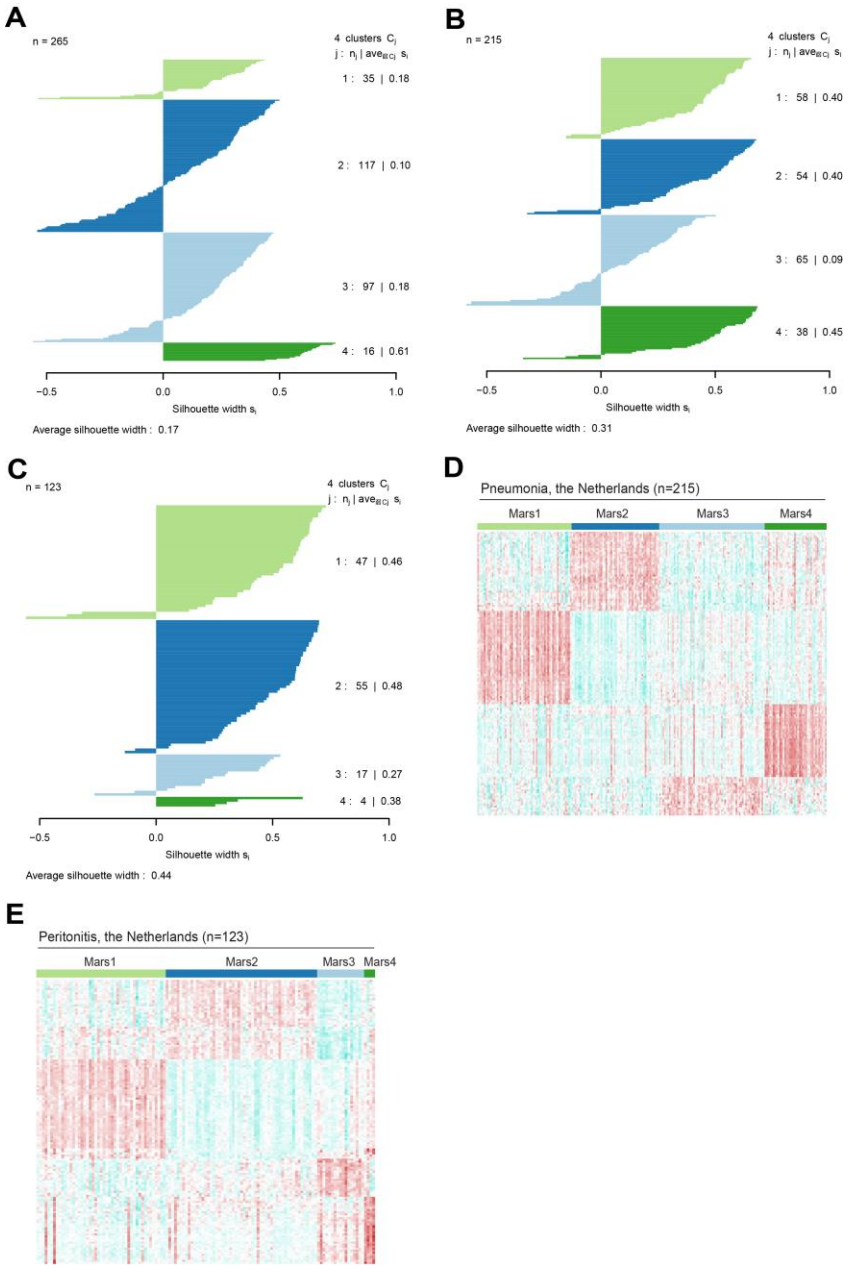

Figure S5. Sepsis molecular endotypes in pneumonia and abdominal sepsis. (**A)** Silhouette widths of community-acquired pneumonia patients from the UK cohort (E-MTAB-4421, n=265) classified to Mars endotypes. (**B, C**) Silhouette widths of the two Dutch cohorts combined (discovery and first validation) diagnosed as (**B**) pneumonia (n=215) and (**C**) peritonitis (n=123); patients with both pneumonia and peritonitis were excluded from this analysis. (**D, E**) Heatmap representation of 140 gene expression indices (rows) and patient samples stratified according to molecular endotype membership (columns) diagnosed at ICU admission with (**D**) pneumonia, or (**E**) peritonitis.

Figure S6

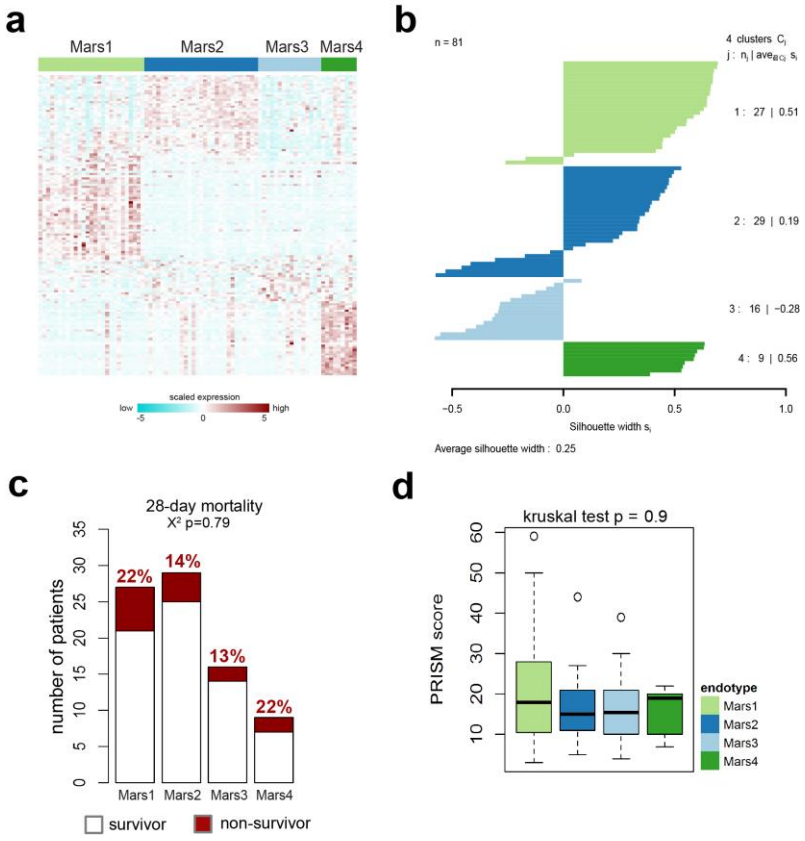

Figure S6: Prediction and classification of blood molecular endotypes in pediatric sepsis. **(a)** Random forest prediction of sepsis endotypes in the pediatric sepsis cohort, USA (GSE13904; n=81)**.** Heatmap depicts the 140 gene classifier (rows) **(b)** Silhouette widths of pediatric sepsis patient samples classified to Mars endotypes. **(c, d)** Endotypes were evaluated for their association to **(c)** 28-day mortality (binary handled), and **(d)** pediatric risk of mortality (PRISM) scores.

Figure S7

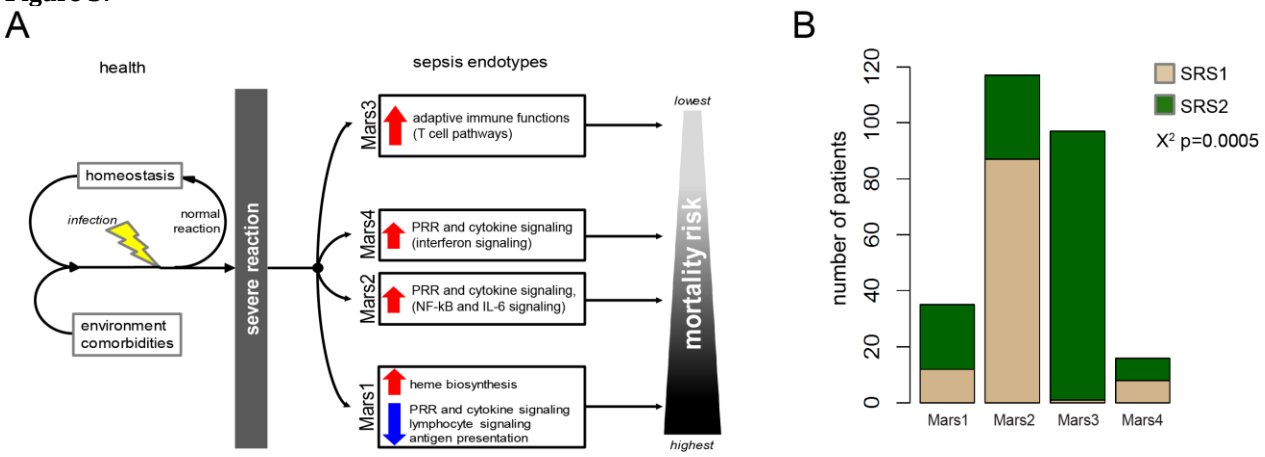

Figure S7. Blood molecular endotype model of sepsis and evaluation of association to "sepsis response states". (**A**) A molecular endotype model for the risk stratification of critically ill patients with sepsis. The relatively high-risk Mars1 sepsis endotype was defined by elevated expression of heme biosynthesis genes concomitant with pronounced under-expression of pattern recognition receptor, cytokine signaling, lymphocyte signaling and antigen presentation pathways. PRR, pattern recognition receptor. (**B**) Stratification of community-acquired pneumonia patients from the UK GAinS cohort by sepsis endotype (Mars1-4) was evaluated for the association to sepsis response signatures 1 and 2 (SRS1 and 2). X^2 p, chi-square test probability.

Figure S8

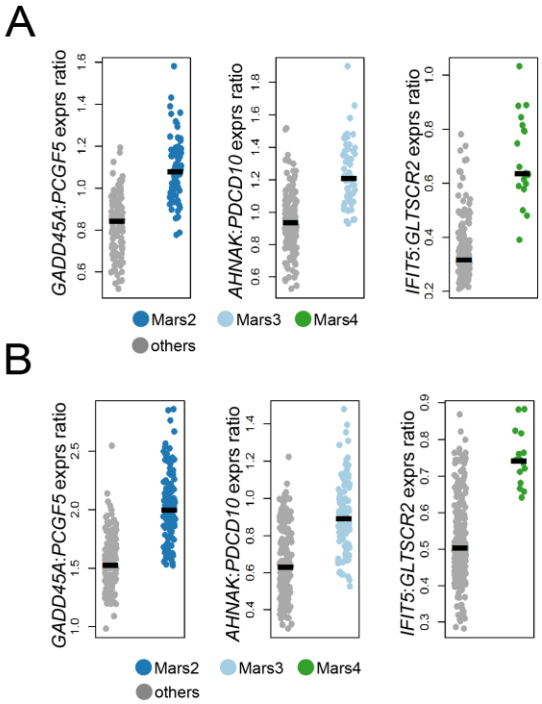

Figure S8. Candidate sepsis endotype biomarker assessment in two validation cohorts. (**A**) Dot plots of Mars2 (*GADD45A:PCGF5*), Mars3 (*AHNAK:PDCD10*) and Mars4 (*IFIT5:GLTSCR2*) scores in the first validation cohort from the Netherlands, and (**B**) in the second validation cohort from the UK. *GADD45A*, growth arrest and DNA damage inducible alpha; *PCGF5*, polycomb group ring finger 5; *AHNAK*, AHNAK nucleoprotein; *PDCD10*, programmed cell death 10; *IFIT5*, interferon induced protein with tetratricopeptide repeats 5; *GLTSCR2*, glioma tumor suppressor candidate region gene 2. Horizontal black line denotes median.

Appendix 2

The data presented herein represent changes in classifier gene expression per endotype (Mars1-Mars4) relative to healthy subjects. logFC denotes the log2 transformed fold difference; adj.P.Val denotes the Benjamini-Hochberg multiple comparison adjusted P-value (adjusted for 24646 probes)

gene	logFC_ Mars1	adj.P.Val_ Mars1	logFC_ Mars2	adj.P.Val_ Mars2	logFC_ Mars3	adj.P.Val_ Mars3	logFC_ Mars4	adj.P.Val_ Mars4
ABCC13	3.178	2.03E-39	0.150	0.500804531	0.872	0.000139066	1.014	7.28E-05
ACVR1B	0.839	5.95E-16	1.680	1.74E-50	0.732	6.22E-12	1.186	5.27E-22
AHNAK	-2.002	4.03E-31	-2.214	1.13E-38	-0.880	1.50E-07	-2.381	3.48E-32
APOL1	-0.537	0.000483136	-0.676	5.54E-06	-0.089	0.630767246	1.347	1.81E-13
APOL2	-1.156	6.74E-11	-0.952	1.91E-08	-0.245	0.211926164	1.343	7.82E-11
APOL6	-0.343	0.020161843	-0.421	0.003206256	-0.018	0.924814717	1.677	6.71E-21
BNIP3L	0.921	3.50E-17	-0.568	3.15E-08	-0.049	0.70394898	-0.067	0.626561234
BPGM	4.116	5.79E-45	0.686	0.006056302	1.302	1.38E-06	1.756	6.57E-09
C5orf56	-0.319	0.003030105	-1.143	1.82E-25	-0.445	8.63E-05	0.505	6.68E-05
CA1	4.823	2.13E-41	1.343	1.30E-05	2.178	8.76E-11	2.282	1.23E-09
CARM1	0.683	1.17E-05	-1.229	1.31E-15	-0.049	0.80195831	-0.419	0.02482907
CCDC176	3.253	8.92E-42	0.013	0.954654047	0.599	0.008770976	0.670	0.008499099
CD59	2.131	4.02E-36	2.897	1.31E-59	1.287	4.41E-15	2.912	1.08E-45
CD74	-2.521	1.93E-60	-2.578	5.88E-66	-1.490	1.81E-26	-1.893	4.09E-32
CD82	0.542	5.98E-06	1.503	3.18E-33	0.627	5.82E-07	0.877	5.09E-10
CECR1	-2.596	8.90E-32	-2.563	3.55E-33	-0.981	4.72E-06	-2.125	5.41E-18
CLEC4D	4.658	1.61E-63	5.645	4.71E-85	3.209	7.97E-36	4.976	1.83E-56
CMPK2	0.189	0.471845857	-0.757	0.002138417	-0.378	0.184260812	2.923	3.41E-21
CTNNAL1	1.833	8.92E-48	0.386	0.000271796	0.410	0.000401803	0.623	1.37E-06
CUTC	0.475	9.97E-06	1.372	4.64E-34	0.452	6.53E-05	0.823	8.64E-11
DACH1	1.354	1.42E-17	2.816	9.90E-58	1.184	3.24E-13	1.731	1.52E-20
DCAF12	1.327	2.34E-13	-0.777	5.75E-06	-0.037	0.869190059	-0.094	0.688220685
DCUN1D1	2.646	8.63E-53	0.673	2.29E-06	0.812	1.55E-07	1.131	8.24E-11
DDX58	-0.906	3.89E-05	-0.540	0.011844832	-0.163	0.530087995	2.043	7.42E-15
DDX60	-1.504	2.80E-08	-1.154	8.89E-06	-1.053	0.000206579	2.305	5.33E-13
DDX60L	0.408	0.004093838	0.913	4.43E-11	0.507	0.000745805	1.935	7.07E-28
DGKZ	-1.547	3.92E-44	-1.425	1.39E-41	-0.593	8.14E-09	-1.325	1.24E-27
DHRS9	2.130	6.73E-19	3.057	6.01E-36	0.832	0.000668855	3.027	3.35E-26
DPP7	-1.448	2.39E-33	-1.339	1.93E-31	-0.584	4.70E-07	-1.526	1.49E-28
DTX3L	-0.693	5.71E-07	-0.372	0.005635301	-0.053	0.752403137	1.200	2.63E-13
ENTPD7	1.371	6.51E-12	2.947	1.83E-43	0.677	0.001150251	1.480	1.73E-10
EPSTI1	-1.089	0.002258763	-1.424	3.63E-05	-0.112	0.800378528	3.291	1.07E-14
ESYT1	-2.748	9.54E-54	-2.465	5.20E-49	-1.527	8.88E-21	-2.711	1.78E-42
FAM104A	1.444	2.55E-25	-0.626	7.63E-07	0.055	0.729567773	0.061	0.724333148
FAM117A	0.805	1.10E-10	-0.994	3.29E-16	-0.334	0.011316023	-0.227	0.132151987

FAM46C	2.799	1.70E-22	-0.648	0.015086758	0.518	0.084212078	0.383	0.261404874
FBXO6	0.302	0.077612839	0.901	4.12E-08	0.547	0.002410381	2.560	8.80E-33
FBXO7	0.793	4.15E-07	-1.159	4.16E-14	-0.326	0.055344741	-0.421	0.024425555
FBXW2	0.368	0.003532736	1.357	6.16E-26	0.290	0.034110519	0.228	0.141381354
FECH	3.057	8.16E-30	-0.364	0.143264811	0.597	0.027448064	0.585	0.053468109
FGFR1OP 2	2.425	6.48E-36	0.327	0.059561745	0.546	0.003632429	0.799	0.000117847
FYN	-2.106	1.12E-40	-2.209	2.36E-46	-1.190	2.13E-15	-2.041	9.72E-31
GADD45A	3.989	3.53E-78	4.528	2.01E-95	2.439	1.75E-38	3.706	1.42E-58
GALNT2	0.639	0.000164595	2.278	9.16E-37	0.593	0.000980242	1.155	7.41E-09
GBP1	-1.480	2.19E-07	-1.436	1.82E-07	-0.612	0.048091994	2.169	1.06E-10
GBP5	-2.110	2.47E-13	-2.174	5.69E-15	-1.312	9.78E-06	1.592	1.61E-06
GCLM	1.842	4.66E-38	2.295	1.79E-55	0.942	4.44E-12	2.004	2.62E-34
GIMAP1	-2.169	1.17E-41	-2.385	9.95E-51	-1.289	3.24E-17	-1.988	6.75E-29
GLRX5	2.228	3.99E-26	-0.336	0.086127563	0.552	0.009331935	0.392	0.105163784
GLTSCR2	-1.761	5.82E-37	-1.853	2.19E-42	-0.996	7.50E-14	-2.192	8.40E-41
GMPR	2.047	5.02E-19	-0.752	0.00044512	0.457	0.058263758	0.212	0.453454964
GNAQ	0.733	2.53E-12	1.494	1.95E-41	0.656	1.27E-09	0.901	1.71E-13
GSPT1	1.635	3.33E-17	-1.060	6.16E-09	0.004	0.988709822	-0.279	0.232523514
GYPA	3.601	2.41E-43	0.375	0.100560726	0.976	5.82E-05	1.285	2.11E-06
HAGH	0.822	1.02E-11	-0.827	1.24E-12	-0.113	0.414382071	-0.225	0.122170985
HERC5	-1.084	2.80E-05	-1.262	4.62E-07	-0.499	0.078865085	2.459	1.87E-15
HK3	2.119	4.28E-43	3.280	1.80E-81	1.908	4.30E-35	2.473	3.41E-43
HLA-DMA	-2.773	1.16E-46	-2.731	1.89E-48	-1.298	3.72E-13	-2.183	1.10E-25
HLA-DPB1	-3.032	6.20E-51	-3.244	2.67E-59	-1.779	2.63E-21	-2.691	3.56E-34
HLA-DRB1	-2.853	1.17E-46	-2.776	1.29E-47	-1.416	1.66E-14	-2.234	1.91E-25
HVCN1	-2.770	6.37E-50	-2.706	2.91E-51	-1.341	4.41E-15	-2.503	2.36E-34
IDI1	2.333	2.53E-25	3.400	6.09E-48	1.011	5.37E-06	2.983	1.94E-29
IFI35	-0.314	0.05658032	0.381	0.016883913	0.165	0.382062873	1.928	3.76E-22
IFI44	0.216	0.490390683	0.116	0.714922241	0.364	0.288224697	4.317	3.99E-30
IFI44L	-0.339	0.292392645	-0.471	0.130901991	0.121	0.753396313	3.906	4.14E-24
IFIH1	-1.816	1.24E-12	-1.600	6.25E-11	-0.823	0.00202468	1.545	1.63E-07
IFIT2	-2.447	2.77E-13	-2.477	1.74E-14	-1.110	0.001432802	1.615	2.87E-05
IFIT3	-1.755	2.10E-07	-2.189	2.64E-11	-0.545	0.144677837	2.509	2.66E-10
IFIT5	-0.408	0.04260343	-0.371	0.059707172	-0.086	0.7250996	2.503	2.62E-24
IRF7	-0.292	0.07127472	0.088	0.596822222	0.387	0.025270601	2.073	1.05E-25
ISCA1	3.210	6.44E-48	0.673	0.000287637	1.021	3.91E-07	1.089	1.34E-06
KPNA4	0.696	3.60E-08	1.365	2.00E-26	0.010	0.951478652	1.093	2.44E-13
LIN7A	1.759	9.90E-31	2.892	1.16E-66	1.698	1.60E-27	2.046	1.10E-30
LOC100131541	-2.186	4.20E-38	-2.069	2.78E-37	-0.796	6.85E-07	-1.654	3.32E-19
LPXN	-2.067	2.34E-50	-1.717	6.47E-41	-0.971	1.75E-14	-1.909	7.40E-36

LRPAP1	0.553	1.90E-07	1.666	1.07E-46	0.862	1.57E-14	1.047	1.40E-16
MAPRE1	0.419	0.000561318	1.462	4.54E-31	0.307	0.018940345	0.800	2.16E-08
METTL9	2.178	3.12E-60	2.541	1.72E-77	1.472	1.17E-32	1.936	3.07E-41
MFF	0.700	2.09E-08	1.756	6.67E-40	0.644	7.44E-07	1.137	1.42E-14
MKRN1	1.519	7.29E-24	-0.247	0.080067166	0.296	0.057772864	0.256	0.144567693
MMP8	4.580	4.20E-27	5.869	2.74E-42	2.021	1.34E-06	3.794	1.66E-15
MPP1	1.615	1.98E-40	0.375	0.000345223	0.579	3.69E-07	0.536	2.66E-05
MSRA	0.721	9.99E-07	1.894	1.57E-34	0.713	3.87E-06	0.714	3.68E-05
MXI1	2.832	1.94E-49	0.594	0.000207527	0.957	3.64E-08	1.118	9.52E-09
NCOA4	0.605	5.87E-10	-0.868	2.28E-19	-0.256	0.01368317	-0.528	3.35E-06
NEDD4	0.789	5.34E-13	1.351	2.29E-33	0.287	0.012686783	0.791	3.99E-10
NLRC4	2.037	1.92E-29	3.346	2.70E-64	1.876	1.97E-24	2.309	2.92E-28
OPTN	0.861	5.45E-07	-1.360	8.78E-16	-0.331	0.077936719	-0.337	0.106995031
PARP14	-1.997	3.53E-20	-1.759	1.81E-17	-0.627	0.00480716	0.879	0.000346555
PARP9	0.068	0.677266097	0.664	9.90E-06	0.494	0.002783235	2.102	1.42E-27
PCGF5	0.465	0.007014733	-1.639	2.97E-21	-0.560	0.002250901	-0.385	0.06552605
PCYT1A	0.701	5.64E-08	1.991	1.44E-45	0.627	3.28E-06	1.180	1.32E-14
PDCD10	2.396	4.07E-44	2.187	5.68E-41	1.149	7.83E-13	2.165	4.78E-30
PFKFB2	4.007	6.56E-40	5.206	2.82E-61	2.090	3.52E-13	4.171	1.16E-33
PGD	1.480	1.05E-26	2.746	1.68E-69	1.662	1.89E-30	1.931	5.39E-32
PGM2	0.496	3.18E-05	1.401	6.04E-30	0.430	0.000650482	0.523	0.000195041
PHOSPHO1	0.348	0.043835215	-1.661	6.43E-22	-0.390	0.035684334	-0.570	0.005131223
PIP4K2A	1.738	5.28E-23	-0.429	0.008352363	0.204	0.282259627	-0.004	0.987421765
PLEKHO1	-1.693	2.64E-27	-1.730	4.10E-30	-0.538	0.000517327	-1.194	6.24E-12
PPM1A	1.470	1.83E-36	0.097	0.364931738	0.396	0.000389658	0.547	1.08E-05
RAB2B	1.950	4.70E-29	-0.191	0.240148626	0.378	0.031327581	0.443	0.022968728
RALGDS	-0.457	0.000164582	-1.706	1.70E-39	-0.724	1.34E-08	-1.089	4.66E-14
RANBP10	1.407	4.64E-20	-0.589	3.46E-05	-0.003	0.987886473	-0.170	0.362772551
REV3L	-1.456	1.55E-31	-1.051	6.99E-20	-0.324	0.008611591	-1.035	4.40E-14
RILP	1.117	5.03E-15	-0.769	1.24E-08	0.254	0.097467267	0.205	0.236006709
RIOK3	2.546	5.21E-49	0.697	1.49E-06	0.657	3.04E-05	0.993	1.73E-08
RNF14	1.640	2.98E-26	-0.121	0.413578463	0.008	0.967608869	0.178	0.330117012
RNF213	-0.929	2.17E-10	-0.490	0.000458755	-0.113	0.504717991	1.047	8.29E-10
RTP4	-0.721	0.000202608	-0.710	0.000154658	-0.267	0.22150827	2.411	4.71E-24
SAMD9L	-0.372	0.083042015	0.099	0.657296069	0.173	0.487482005	2.552	9.75E-23
SEC62	2.137	1.64E-36	1.821	2.56E-30	0.761	2.40E-06	1.482	7.59E-16
SEPT9	-2.363	1.62E-71	-1.845	9.03E-55	-1.241	5.08E-27	-2.209	1.72E-53
SERPING1	-0.215	0.395955028	-0.523	0.030006746	0.174	0.549390526	3.312	2.17E-27
SESN3	2.630	3.13E-27	-0.201	0.387309536	0.688	0.004710758	0.853	0.001582541
SGTB	0.812	3.65E-11	1.932	1.35E-47	0.728	9.79E-09	1.082	5.61E-14
SLC14A1	2.638	2.86E-37	0.012	0.95110274	0.550	0.005884479	0.515	0.021665355

SLC25A38	0.001	0.99302085	-1.495	5.09E-32	-0.611	1.75E-06	-1.044	5.35E-13
SLC25A39	0.454	0.006236466	-1.304	1.69E-15	-0.281	0.125293438	-0.457	0.021663262
SLC4A1	1.985	7.24E-14	-1.139	5.61E-06	0.177	0.565922628	-0.161	0.636319057
SPTB	2.596	1.75E-34	-0.115	0.566171753	0.764	0.000185723	0.538	0.020400315
ST6GALNAC4	1.016	2.97E-08	-1.373	1.82E-14	0.014	0.952430955	-0.343	0.12376709
STAT1	-1.350	4.35E-12	-1.127	1.43E-09	-0.836	3.39E-05	1.189	1.31E-07
STOM	3.277	3.77E-57	3.564	1.41E-67	1.700	5.64E-20	3.039	2.01E-41
TAP1	-1.016	1.54E-13	-0.572	1.10E-05	-0.225	0.131770996	0.995	3.90E-10
TAP2	-1.604	1.05E-17	-1.289	3.87E-13	-0.478	0.013923086	0.723	0.00073416
TDRD7	-0.051	0.693504437	0.769	1.18E-10	0.214	0.112958973	1.716	3.78E-29
TRIM22	-0.212	0.284031679	0.261	0.176404885	-0.102	0.661584401	2.135	7.66E-20
TRMT6	0.316	0.022013946	1.496	1.75E-26	0.122	0.446216289	0.397	0.015669047
TRNAU1AP	0.186	0.156065724	1.464	4.02E-28	0.444	0.001206981	0.591	0.000106127
TRPS1	0.474	0.000153958	1.583	1.62E-33	0.461	0.000501276	0.820	2.63E-08
TSPO	1.222	6.06E-27	2.022	2.66E-60	1.248	2.21E-26	1.147	5.58E-19
UBE2F	1.938	1.07E-50	1.556	3.55E-39	0.772	4.53E-11	1.653	5.28E-32
UBE2H	1.948	8.80E-38	1.356	1.01E-22	0.268	0.073621636	1.032	1.74E-10
UBE2L6	-1.411	6.79E-16	-1.532	1.83E-19	-0.576	0.001392453	0.885	9.38E-06
USP25	-0.862	2.31E-12	-0.278	0.018451215	-0.349	0.006807241	0.600	2.35E-05
VTI1B	1.328	1.06E-33	-0.031	0.772132675	0.315	0.003191182	0.198	0.10729814
XAF1	-0.575	0.00314094	-0.625	0.000919368	-0.221	0.321657265	2.389	1.42E-23
XK	4.247	1.52E-49	1.001	2.88E-05	1.795	6.72E-12	2.206	7.25E-14
XRN2	-0.443	7.06E-05	0.623	8.59E-09	-0.054	0.687964994	0.013	0.929856881
ZFP36L2	-2.406	1.12E-39	-2.218	2.58E-37	-0.929	6.47E-08	-2.128	6.54E-26